This item is the archived peer-reviewed author-version of: Experimental investigation of granule size and shape dynamics in twin-screw granulation

Authors: Kumar A., Vercruysse J., Bellandi G., Gernaey K.V., Vervaet C., Remon J.P., De Beer T., Nopens I.

In: International Journal of Pharmaceutics, 475(1-2), 485-495 (2014)

Experimental investigation of granule size and shape dynamics in twin-screw granulation

Ashish Kumar[a,b], Jurgen Vercruysse[c], Giacomo Bellandi[a], Krist V. Gernaey[d], Chris Vervaet[c], Jean Paul Remon[c], Thomas De Beer[b,1], Ingmar Nopens[a,*]

[a]*BIOMATH, Dept. of Mathematical Modelling, Statistics and Bioinformatics, Faculty of Bioscience Engineering, Ghent University, Coupure Links 653, B- 9000 Gent, Belgium*
[b]*Laboratory of Pharmaceutical Process Analytical Technology, Dept. of Pharmaceutical Analysis, Faculty of Pharmaceutical Sciences, Ghent University, Harelbekestraat 72, B-9000 Ghent, Belgium*
[c]*Laboratory of Pharmaceutical Technology, Dept. of Pharmaceutics, Faculty of Pharmaceutical Sciences, Ghent University, Harelbekestraat 72, B-9000 Ghent, Belgium*
[d]*CAPEC-PROCESS, Dept. of Chemical and Biochemical Engineering, Technical University of Denmark, DK-2800 Kongens Lyngby, Denmark*

[*]Email address: ingmar.nopens@ugent.be, Tel.: +32 (0)9 264 61 96; fax: +32 (0)9 264 62 20
Email addresses: ashish.kumar@ugent.be (Ashish Kumar), jurgen.vercruysse@ugent.be (Jurgen Vercruysse), giacomo.bellandi@ugent.be (Giacomo Bellandi), kvg@kt.dtu.dk (Krist V. Gernaey), chris.vervaet@ugent.be (Chris Vervaet), jeanpaul.remon@ugent.be (Jean Paul Remon), thomas.debeer@ugent.be (Thomas De Beer)
URL: www.biomath.ugent.be (Ingmar Nopens)
[1]Shared last authorship

Preprint submitted to International Journal of Pharmaceutics *September 19, 2014*

Abstract

A twin-screw granulator (TSG), a promising equipment for continuous high shear wet granulation (HSWG), achieves the desired level of mixing by a combination of the appropriate screw configuration and a suitable set of process settings (e.g. feed rate, screw speed, etc.), thus producing a certain granule size and shape distribution (GSSD). However, the primary sizing and shaping mechanism behind the resulting distribution is not well understood due to the opacity of the multiphase system in the granulator. This study experimentally characterised the GSSD dynamics along the TSG barrel length in order to understand the function of individual screw modules and process settings, as well as their interaction. Particle size analysis of granules collected at the outlet of the TSG suggested significant interaction between the process and screw configuration parameters influencing the heterogeneity in the GSSD. By characterising the samples collected along the screw length, a variable influence of the screw modules at different process conditions was observed. At low liquid-to-solid ratio (L/S), the first kneading module seemed to play a significant role in mixing, whereas the second kneading module was found to be more involved in reshaping the granules. At high L/S and high throughput, aggregation mainly took place in the second kneading module changing the GSSD. The results obtained from this study will be further used for the calibration and validation of a mechanistic model and, hence, support future development of a more detailed understanding of the HSWG process in a TSG.

Keywords: twin-screw granulation, continuous pharmaceutical production, granule size and shape analysis

1. Introduction

Granulation is a process aiming at enlarging powder particles, which can be advantageous for many reasons. The size enlargement results in gravity forces exceeding the van der Waals forces, thereby contributing to better flow properties required for improved processability and accurate dosing in further downstream processing. Especially in the pharmaceutical industry, where often highly potent drugs are processed, the amount of dust generated by powder handling is reduced by granulation, resulting in improved safety. Also, segregation (demixing) can be minimized along with the improved downstream processing characteristics of the granules. Therefore, wet granulation is an important process for the particle enlargement during the formulation of solid dosage forms in the pharmaceutical industry (Ennis, 2010). Vervaet and Remon (2005) extensively reviewed continuous granulation techniques. The high shear twin-screw granulation system has received most attention in the last decades due to its inherent benefits, including ease of use in continuous operation and the potential to integrate the TSG with other operations (Kumar et al., 2013). The high shear wet granulation (HSWG) process in the twin-screw granulator (TSG) can be divided into several stages (Fig. 1). A number of different mechanisms, including nucleation, growth, aggregation, and breakage, which ultimately determine the characteristics of the produced granules, typically drive the dynamics of wet granulation. Although details about the precise sequence of growth and breakage mechanisms during TSG are not available from the literature, growth and breakage of granules are expected to occur simultaneously due to the inhomogeneous shear force distribution inside the TSG barrel (Dhenge et al., 2012).

[Figure 1 about here.]

Normally in batch HSWG the granulation time is in the order of minutes, while, in a TSG, it is limited to a few seconds (Kumar et al., 2014). The short granulation time is, although desirable from the productivity point of view, challenging for micro to meso scale rate processes in HSWG (Fig. 1). The rate processes of wet granulation are required to occur during the short granulation time before the material leaves the TSG. Thus, besides a homogeneous distribution of granulation liquid and powder, the wet mixing in a TSG is also required to be achieved within the shortest possible screw length and with minimum power input. To facilitate wet granulation, the TSG screw is composed of mainly two blocks (Fig. 2). The first and the larger component contains the inter-meshing conveying elements involved in transport of the dry and then wetted powder. The second component is the mixing section, which contains kneading discs staggered at a certain angle to cause restriction to the flow and hence provide the required mixing for wet granulation. These modules change the shear environment of the material being conveyed, which determines the final granule characteristic distribution, such as granule size and shape distribution (GSSD), granule strength, etc. (Djuric et al., 2009). Besides the functional role of the screw configuration, performance of a TSG is also related to the applied process parameters. Along with the screw speed and the screw configuration, the feeding rate of the powder and the granulation liquid which together determine the liquid-to-solid ratio (L/S), and the fill ratio inside the barrel are the main process parameters. Therefore, they can be independently chosen to achieve the desired mixing levels of the powder and the granulation liquid, and influence the granulation yield at the outlet (Vercruysse et al., 2012, 2013).

[Figure 2 about here.]

However, there is very little understanding regarding the primary shaping mechanisms behind the particle size and shape distribution in the TSG during wet granulation, due to the opacity of the multiphase system (Dhenge et al., 2012; El Hagrasy and Litster, 2013). Most of the studies rely on the characterisation of the granules from the outlet of the TSG. Furthermore, the measured torque of the granulator drive is used as the steady state criterion in most studies using TSG. However, torque being a 0-dimensional measurement does not provide information linking the role of change in process parameters to the role of individual screw elements in the TSG.

This study extends the spatial dimension of knowledge regarding HSWG using TSG in order to understand the dynamic change in characteristics of the material while progressing in the TSG barrel. The purpose of this study was to experimentally characterise the change in GSSD along the TSG barrel in order to understand the function of individual screw modules and their interaction with other process parameters such as L/S, screw speed and filling degree in the TSG.

2. Materials and methods

2.1. Pharmaceutical model formulation

In this study, a premix of α-Lactose monohydrate (Pharmatose 200M, Caldic, Hemiksem, Belgium) and Polyvinylpyrrolidone (PVP) (Kollidon® 30, BASF, Ludwigshafen, Germany) (ratio: 97.5/2.5, w/w) was granulated with distilled water using the ConsiGma-1 continuous wet granulation system.

2.2. Continuous twin screw granulation

Granulation experiments were performed using a 25 mm diameter co-rotating TSG with option to open the barrel, which is the granulation module of the ConsiGma-1 unit (GEA Pharma Systems, Collette™, Wommelgem, Belgium). The granulator screws had a length-to-diameter ratio of 20:1 (Fig. 2). The screw configurations up to 6 kneading discs (Length = Diameter/4 for each kneading disc) were composed of one kneading block. For the screw configuration with 12 kneading discs, two kneading blocks each consisting of 6 kneading discs were used. Both kneading zones were separated by a conveying screw block (Length = 1.5 Diameter). The stagger angle of the kneading elements was fixed at 60°. An extra conveying element (Length = 1.5 Diameter) was implemented after the second kneading block together with 2 narrow kneading discs (L = D/6 for each kneading disc) in order to reduce the amount of oversized agglomerates, as reported by Van Melkebeke et al. (2008). The barrel jacket temperature was set at 25°C. The TSG barrel had a feed segment, where the powder entered the barrel and was transported through the conveying zone to the work segment, where the granulation liquid was added to the powder (Fig. 2) (Fonteyne et al., 2012; Vercruysse et al., 2012). During processing, the powder premix was gravimetrically fed into granulator by using a twin concave screw feeder with agitator (DDW-MD2-DDSR20, Brabender, Duisburg, Germany). Distilled water as granulation liquid was pumped into the screw chamber using a peristaltic pump (Watson Marlow, Comwall, UK) using silicon tubings connected to 1.6 mm nozzles. The granulation liquid was added before the first kneading disc by dripping through two liquid feed ports, each port located just above each screw in the barrel. The wetted, but not yet mixed powder was forced to follow a granulation track composed of the two co-rotating screws with a number of transport and mixing modules based on screw configuration. As the wet powder progresses along the length of the granulator, the distribution of particle characteristics changes.

2.3. Experimental design and sample preparation

A full factorial experimental design was performed to evaluate the influence of number of kneading discs (2, 4, 6, 12), screw speed (500-900 rpm), throughput (10-25 kg/h) and L/S (4.58-6.72% (w/w) based on wet mass) (Table 1). Three center point experiments were performed as well, resulting in 32 + 3 = 35 experiments. For each run, samples were collected from different locations inside the barrel by opening the barrel after stopping the process running at steady state (Fig. 2). Sample location 1 was just prior to the first kneading block, sample location 2 on the first kneading block, sample location 3 was between the first and second kneading block, sample locations 4 and 5 were on and right after the second kneading block. Irrespective of the number of kneading blocks, sample locations on the screw were kept constant during sampling. Sample location 6 was the regular outlet of the granulator and, hence, a large amount of granules was available at that location. The wet granules from all the experiments were dried at room temperature for 24 h and their GSSD was classified in granules size fractions <150, between 150-1000 and >1000 µm (Table 1). The particle size distribution of α-Lactose monohydrate used for this study was 90% not more than 100 µm and 100% not more than 200 µm. Therefore <150micron was defined as fine to prevent under-prediction of fines. Since several responses were measured, it was helpful to fit a model simultaneously representing the variation of all responses to the variation of the factors. Therefore, the partial least squares (PLS) method was used (employing Modde 9.0 software by Umetrics, Umeå, Sweden), which is able to deal with many responses simultaneously, accounting for their covariances. The effect plot was used to show the change in the response when a factor vary from low to high level, keeping other factors at their averages. The respective 95% confidence interval is shown for each plot. Insignificant effects are those where the confidence interval includes zero. The effects in this plot are ranked from the largest to the smallest.

[Table 1 about here.]

2.4. Determination of torque

The TSG has an inbuilt torque gauge and the achievement of steady-state was decided based on the equilibration of the measured torque of the granulator. The torque values obtained after equilibration of the process were averaged to give the overall torque at steady-state during each run. The drive motor torque values are an indication of the shear and consolidation forces experienced by materials inside the barrel.

2.5. Characterisation of granules

2.5.1. Sieve test for particle size analysis

The granule size distribution (GSD) of the granule samples, collected at the outlet of the TSG (sample location 6 in Fig. 2) during each design experiment, was determined using the sieve analysis method (Retsch VE 1000 sieve shaker (Haan, Germany)). Granule samples (100 g) were placed on a shaker for 5 min at an amplitude of 2 mm using a series of sieves (150, 250, 500, 710, 1000, 1400 and 2000 µm). The amount of granules retained on each sieve was determined. All granule batches were measured in triplicate. The fractions <150, 150-1000 and >1000 µm were defined as the amount of fines, fraction of interest for tableting and oversized fraction, respectively.

2.5.2. Dynamic image analysis for size and shape analysis of granules

The GSSD of the samples from sampling locations which were inside the TSG barrel (Fig. 2), were determined via dynamic image analysis (DIA) used in the EyeTech instrument (Ankersmid B.V., Oosterhout, The Netherlands). A high speed camera (Fig. 3a) records pictures (up to 30 pictures /sec) and visualises the particle distribution in real time during the measurement. The camera was synchronized with a pulsing light emitting diode (LED) and takes backlighted images. The captured images of flowing powders were used to calculate GSSD.

The average Feret diameter was used as the size parameter that provides information on a diameter that is measured every 5 degrees, resulting in an average of a total of 36 diameters for each granule (Fig. 3b, eq. 1). This size information also serves as a basis for the calculation of shape related parameters such as the aspect ratio, which measures the elongation of the granule and has been used in this study. It is a ratio of the smallest over the largest diameter of the granule (eq. 2). The aspect ratio gives information about how far the particles deviate from being spherical. Rod shaped particles have an aspect ratio less than 0.5 while an aspect ratio close to 1 indicates higher sphericity of the granules.

$$\text{Feret Diameter} = \frac{d_1 + d_2 + d_3 + d_4 \ldots d_{36}}{36} \tag{1}$$

$$\text{Aspect ratio} = \frac{\text{Minimum Feret Diameter}}{\text{Maximum Feret Diameter}} \tag{2}$$

[Figure 3 about here.]

The link between mean Feret diameter and aspect ratio of the granules was determined simultaneously by the WINDOX software using Sympatec Image Analysis (QICPIC) (with the same measurement system as the Eyetech) by dispersing the granules under gravity through the focus plane of a high speed camera.

The screw arrangement at sample locations 2 and 4 was changed based on the experimental design, which lead to a deviation in granule characteristics at these locations purely due to the local and experimental run specific conditions. Therefore, they have not been used in the remainder of this study and the samples from location 1, 3 and 5 in Fig. 2 were analysed for further study.

3. Results and discussion

This study examined the impact of four main factors of HSWG using TSG, which include the screw speed, number of kneading discs, throughput and L/S during granulation on the GSSD.

3.1. Influence of process variables on the granules at the outlet

The samples collected at the outlet of the TSG (sample location 6 in Fig. 2) were analysed using a sieve test for each experiment. This was useful to understand the effect of the various factors on the granule size fractions (F) defined as fines (F $<$ 150 µm), fraction of interest for tabletting (150 µm $<$ F $<$ 1000 µm) being the granulation yield, oversized granules (F $>$ 1000 µm) as well as the measured torque (Nm) (Table 1). The effect of individual factors and their combinations on size fractions determined via the PLS method, suggested that the L/S had a significant effect on both the fines (16.10–45.87% $<$ 150 µm) and oversized fraction (15.21–49.43% $>$ 1000 µm) of the granules (Fig. 4, Table 1). From this analysis, it was observed that granules contained a higher fraction of fines when the powder was less wetted at low L/S and vice versa produced more oversized granules. Since the parameters having a positive effect on the oversized fraction had a negative effect on the fines and vice versa, these parameters did not affect the yield of the fraction of interest significantly (yield between 31.01 - 55.90%). Furthermore, low screw speeds resulted in an increase of the oversized fraction, due to material accumulation at a reduced conveying rate and the lack of proper sheared mixing and less breakage inside the barrel. For the oversized fraction, the interaction between L/S and number of kneading discs was significant as the effect of the change in L/S was observed to be different at a low or high number of kneading discs. At a higher number of kneading discs, L/S variations caused more drastic changes in the oversized fraction compared to similar L/S variations for a low number of kneading elements.

The measured torque of the granulator drive, which is related to the fill level and the shear mixing of material in the TSG, was found to be most affected by the number of kneading discs. The increase in the number of kneading discs caused an enhanced hindrance to the flow of material and hence a high torque of the granulator drive. However, this hindrance to the flow in the screw channel resulted in a greater residence time and more distributive mixing of the powder which is essentially required for a better granulation yield (El Hagrasy and Litster, 2013). Also, the interaction between the number of kneading elements and screw speed was significant with respect to the torque. The torque increase from 2 to 12 kneading elements was higher at a low screw speed compared to that at a high screw speed. This could be explained by the higher filling degree of the barrel at low screw speed.

[Figure 4 about here.]

3.2. Influence of process variables on granule properties along the TSG length

The samples from location 1 (before the first kneading block), location 3 (after the first kneading block) and location 5 (after the second kneading block in the screw configuration with 2 kneading blocks) were used to characterise the change in the GSSD along the TSG length (Fig. 2). Firstly, it is important to point out that the granulation using only 2 kneading discs did not yield a sufficient degree of control over the process, and therefore the results were inconsistent (data not shown). We believe that 2 kneading discs in the screw configuration pose a too low hindrance to the flow in the screw channel. Due to this, the primary response by the kneading block in terms of restriction to the flow was significantly asynchronous, thus generating random results. Therefore, for further comparison only results from runs with 4, 6 and 12 kneading discs are presented. The pattern of evolution in granule size and shape indicates that the formation of primary granules (50-200 μm) led to a loss in the particle shape uniformity via reduction in the aspect ratio (Fig. 5). The further growth of granule size (between 200-400 μm) resulted in a more uniform and higher mean aspect ratio. However, an increase in granule size beyond 400 μm led to a more heterogeneous and relatively lower aspect ratio. For the three sample locations (1, 3 and 5) in Fig. 2 it was observed that granules at location 1 (top subplot in Fig. 5) had a reasonably homogeneous aspect ratio except for the oversized granules. As the granules moved to sample location 3 (middle subplot in Fig. 5) both primary (50-200 μm) and oversized granules were further deformed. Compared to location 3, there was a minor increase in the width of the intermediate size granules (between 200-800 μm) at sample location 5 (bottom subplot in

Fig. 5) with a more uniform aspect ratio. However, the larger granules remained deformed. This can be explained by the high shear and the lack of free space inside the TSG which is very different from high-shear mixers where granules, despite their large sizes, tumble on their free surface and get rounded (Lee et al., 2013).

[Figure 5 about here.]

Furthermore, as the wetted powder is conveyed from the pre-kneading zone to the first kneading zone and further, the number density of the granules shifted towards the right, indicating an increase in the fraction of larger granules and occasionally some breakup at the end (Fig. 6 and 8). Remarkably, an increasing number of kneading discs not only increased the fraction of larger granules for the downstream sample locations 3 and 5 which were located after the kneading blocks but also at sample location 1, which was located upstream of the kneading discs. This suggests that along with the mixing section composed of kneading discs, a significant mixing and granulation also occurs in the upstream section. The material in the mixing section flows more slowly than in the upstream section and hence the built-up material in the flow restricted zone of the barrel is force-mixed with the incoming materials. Lee et al. (2012) have shown that the degree of filling of the 'non-kneading zone' of the granulator increases with an increase in the restriction to the flow. Also, elongation of the granules was observed to decrease along the granulator length and for increasing number of kneading discs (Fig. 7 and 9). This spherification of granules together with enlargement now allows discussion of the effects of factors as well as their interactions on GSSD.

3.2.1. Effect of throughput

Low liquid-to-solid ratio (4.58%) and low screw speed (500 rpm)

An increase in the throughput from 10 kg/h to 25 kg/h keeping the L/S and screw speed at the lowest level resulted in a minor increase in the granule size for successive sample locations (comparing ID 1 and 3 plots in Fig. 6). This effect was clearest for 12 kneading discs, where a small reduction in the amount of fines for sample location 5 occurred. No significant effect on the shape distribution was observed for configurations containing up to 6 kneading discs (comparing ID 1 and 3 plots in Fig. 7). For a higher number of kneading discs the elongation of the granules decreased with the progressive sample locations indicating a greater consolidation of granules.

High liquid-to-solid ratio (6.72%) and low screw speed (500 rpm)

At high L/S more granulation liquid enhanced the size enlargement rate processes (such as wetting, nucleation and aggregation), and thereby a shift of GSDs towards higher average diameters was noticed (ID 2 and 4 plots in Fig. 6). For up to 6 kneading discs, increased throughput had a trivial influence on granulation, which was reflected by the fact that no change in the GSD was observed. However, a further granule size enlargement at location 5 and a broadening of the distribution were observed when the second kneading block was present (comparing ID 2 and 4 plots for 12 kneading discs in Fig. 6). Besides the size, increasing throughput at a high number of kneading discs affected the aspect ratio profile, which shifted towards the right and became narrower for location 3 (ID 2 and 4 plots in Fig. 7). However, the higher fill ratio at increased throughput and sluggish flow of more wetted powder in the granulator barrel led to an almost doubled TSG drive torque (ID 4 plots in Fig. 6).

[Figure 6 about here.]

Low liquid-to-solid ratio (4.58%) and high screw speed (900 rpm)

Despite good shear mixing at high screw speed, increasing the throughput did not support an increase in the fraction of larger granules due to a low L/S (ID 1 and 3 plots in Fig. 8). The increased throughput for the 12 kneading discs configuration showed a reduction in the larger granules after the second kneading block (location 3 and 5 profiles when comparing ID 1 and 3 plots for 12 kneading discs in Fig. 8). Besides the reduction in the granule size, the increased throughput did not affect the shape of granules and the profiles for ID 1 and 3 plots in Fig. 9 corresponded to the same pattern for an equal number of kneading discs.

[Figure 7 about here.]

High liquid-to-solid ratio (6.72%) and high screw speed (900 rpm)

With an increase in throughput at these conditions, granulation was more uniform which led to a clear difference between the GSD profile from sample location 1, 3 and 5 when two kneading blocks were used (comparing ID 2 and ID 4 plots in Fig. 8). However, the GSD of location 3 was narrower than at location 5 in the ID 4 plot for 12 kneading discs. The increased throughput only affected the shape of the granules from location 1, where the granulation liquid was distributed to a larger amount of powder available at high throughput. However, due to the high shear-induced mixing at high screw speed, despite the high filling ratio the downstream material was well-mixed thus yielding a more uniform particle aspect ratio distribution for ID 4 plots compared to ID 2 plots in Fig. 9. However, for sample locations 3 and 5 the aspect ratio profile corresponded to the same pattern for an equal number of kneading discs.

The above suggests that increasing throughput is not beneficial without sufficient granulation liquid and shear mixing to make strong bridges between powder particles in the agglomerates. Despite the availability of granulation liquid, when the shear-induced mixing is poor, an inhomogeneous distribution of liquid over the material occurs resulting in a broader GSD. On the other hand, at low L/S, an increase in screw speed leads to a high level of shear mixing and further contributes to the fragility of the granules and thus increased attrition and breakage. Although an increase in throughput requires a higher torque, this issue can be solved by increasing the screw speed during granulation which increases the conveying rate and reduces the load on the screws. At high shear and high L/S, the wet granules are easy to deform leading to a more uniform shape. However, due to the higher filling of the channels of the screws and the increased consolidation at high throughput, attrition of the wet mass between the screws and barrel wall may increase, as observed by Dhenge et al. (2011).

[Figure 8 about here.]

3.2.2. Effect of liquid-to-solid ratio

Low throughput (10 kg/h) and low screw speed (500 rpm)

When the L/S was increased at low levels of throughput and screw speed, the degree of aggregation increased (comparing ID 1 and 2 in Fig. 6). With an increase in the number of kneading discs, the measured torque and shear mixing increased and the GSD shifted towards higher granule sizes at sample locations 3 and 5 (ID 2 plot in Fig. 6). However, no narrowing of the size distribution at sample location 5 was observed. An additional kneading block showed only a slight contribution to the aggregation when comparing the number based GSD profile at sample location 3 and 5 in the ID 2 plots of Fig. 6. This also happened due to the fact that bigger granules are created by aggregation of many small particles, thereby resulting in a visible drop in the number of small size granules, but only a small increase in the bigger ones. The increase in L/S also reduced the granule elongation for the screw configurations with 6 and 12 kneading discs at sample locations 3 and 5 (comparing ID 1 and 2 in Fig. 7). Altogether it can be confirmed that the additional kneading block had a minor contribution in this case, both in terms of granule enlargement and the spherification of granules.

High throughput (25 kg/h) and low screw speed (500 rpm)

When the granulation was performed at high throughput and a low screw speed, an increase in L/S increased the degree of aggregation (comparing ID 3 and 4 plots in Fig. 6). However, the most remarkable change was observed for the screw configuration with 12 kneading discs when the GSD profiles of the three sample locations were clearly segregated by the second kneading block in the TSG. Moreover, the aspect ratio profiles at higher L/S shifted towards the right and became narrower in ID 4 compared to ID 3 plots of Fig. 7, indicating an increased aspect ratio and uniformity of the granule shape. However, the torque of the TSG drive increased significantly due to the high fill ratio and sluggish flow of wetted powder inside the granulator barrel.

[Figure 9 about here.]

Low throughput (10 kg/h) and high screw speed (900 rpm)

With the increase in L/S at the low throughput and high screw speed, there was only a minor increase in granule size for the screw configuration with 4 kneading discs (comparing ID 1 and 2 plots in Fig. 8). However, increasing the number of kneading discs increased the aggregation level due to which the GSD shifted towards a larger diameter. The second kneading block showed only a small contribution to the aggregation level as can be observed from profiles from sample locations 3 and 5 in ID 2 plots of Fig. 8. This may be due to the lack of unwetted powder in the granulator to support further agglomeration. Besides, the additional granulation liquid encouraged the formation of more spherical granules in successive sample locations of the TSG suggesting a higher level of consolidation of the granules (comparing ID 1 and 2 plots in Fig. 9). However, the shape distributions of samples before and after the second kneading block were similar. This indicates that, at a very low fill level, the second kneading block played a minor role in changing the shape of the granules.

High throughput (25 kg/h) and high screw speed (900 rpm)

At high throughput more material was available inside the TSG, but an increase in screw speed caused a reduction in the fill level and improved mixing. However, at a lower number of kneading discs, a considerable reduction of distributive mixing of the powder and the granulation liquid and consequent aggregation occurred, leading to minor shifts in GSD between locations 1, 3 and 5 (comparing ID 3 and 4 plots in Fig. 8). When the number of kneading discs was increased, the wetted powder was well mixed despite a lower fill level of the barrel and hence agglomerated, leading to an increase in granule size. For the screw configuration with 12 kneading discs, the most significant difference between all three locations was observed, which can be attributed to the presence of an additional kneading block between sampling location 3 and 5 along with the one between sample location 1 and 3. An increase in the number of kneading discs also caused an increase in the number density of high aspect ratio granules (comparing ID 3 and 4 plots in Fig. 9). Moving from a low to a high number of kneading discs, for the location 1, 3 and 5 the aspect ratio distributions were very similar. This indicates that shear-induced consolidation occurred in the early stage of the granulation (near location 1) and the aggregation and the consolidation of the granules took place simultaneously.

Overall, more granulation liquid at increased L/S enhances wetting, nucleation and aggregation, i.e. granule enlargement rate processes (Litster and Ennis, 2004). However, an increased L/S can only improve the agglomeration level when the mixing is also increased. An increase in screw speed causes a reduction in the fill level of the wetted material and an increase in the shear leading to improved mixing. Especially at high screw speed the axial mixing inside the granulator increases significantly (Kumar et al., 2014). In this study, a higher L/S also affected the shape of the granules along the length and the produced granules grew to be more spherical. This outcome is in accordance with results reported by Dhenge et al. (2012) comparing samples collected at the granulator output only. However, the torque of the TSG drive increases significantly due to the high fill ratio and sluggish flow of wetted powder in the granulator barrel, which can be reduced by increasing the conveying rate of the screw at high screw speed.

3.2.3. Effect of combined change in throughput and liquid-to-solid ratio

Low screw speed (500 rpm)

When both throughput and the L/S were increased at low screw speed, there was less difference between the GSD from sample locations 1 and 3 for a low number of kneading discs due to the lack of mixing (comparing ID 1 and 4 plots in Fig. 6). However, a progressive mixing in the axial direction occurred due to the shear induced during the conveying of the wet powder, hence changing the morphology in terms of reduction in the fraction of smaller granules and an increase in the fraction of larger granules at sample location 3 and 5 in the ID 4 plot for 4 kneading discs in Fig. 6. For the screw configuration with 12 kneading discs, most distinctly separate distributions for the three sample locations were observed. However, the number density of small granules also increased with spatial progress indicating that, beyond the consolidation, breakage was an important size reduction phenomenon and competed with the aggregation process in the second kneading block of the TSG under these conditions. Also, at a low number of kneading discs, the shape distribution of the sample locations 1, 3 and 5 were similar (comparing ID 1 and ID 4 plots in Fig. 7). For an increasing number of kneading discs, an increase in the aspect ratio of granules from location 3 and 5 caused the shape distribution of the locations 1 and 3 samples to be more distinct, while the difference between locations 3 and 5 samples remained low.

High screw speed (900 rpm)

When the screw speed was increased, for 4 kneading discs the difference between the downstream sample profiles from locations 3 and 5 was small (plot ID 4 in Fig. 8). With 6 kneading discs the restrictive forces started playing a role, which resulted in the formation of more stable GSD even before the material entered the first kneading block (plot ID 4 in Fig. 8). However, in lack of adequate distributive mixing of wetted powder, there was only a minor difference between sample location 3 and 5. When a second kneading block was added between sampling location 3 and 5 in the screw, the powder with high moisture content was distributively mixed and hence agglomerated furthermore (plot ID 4 in Fig. 8). This led to GSD profiles, which were separated for all the three sample locations. Also, unlike the observations at low screw speed (ID 4 plot for 12 kneading discs in Fig. 6), the number density for the lower particle size did not increase with the spatial progress for high screw speed indicating that sufficient mixing occurred to support the aggregation process at location 5 in the TSG barrel (ID 4 plot for 12 kneading discs in Fig. 7). The suitability of this condition was also reflected in the shape dynamics as the increase in number of kneading discs only caused a minor increase in the aspect ratio distributions (comparing ID 1 and ID 4 plots in Fig. 9). For both a low and a high number of kneading discs, for the location 1, 3 and 5 the aspect ratio distribution were quite similar regardless of the throughput. This indicates that consolidation of the granules went well along with the aggregation during the conveying of the granules in the TSG barrel.

These results suggest that increased mixing is required when the throughput and the L/S are high. Since the mixing of the wetted powder inside the TSG is mainly distributive, the most effective mixing in this condition can be obtained by increasing the number of kneading discs. Besides, a high shear and a low fill level due to the increased conveying rate at high screw speed can lead to a very efficient mixing in the TSG barrel (Vercruysse et al., 2012). These results also suggest that at increased shear first the wetted granules' shape changes through consolidation, only after which the breakage occurs.

3.2.4. Effect of increase in screw speed

At low throughput and L/S, when the screw speed was increased from 500 rpm (ID 1 plot of Fig. 6) to 900 rpm (ID 1 plot of Fig. 8), there was no significant shift in the GSDs. Only the measured torque level decreased for 12 kneading discs due to reduction in hindrance to the flow at increased conveying rate and low filling ratio at high screw speed. Comparing the shape dynamics, the distribution of shape followed a consistent pattern due to a lower fill ratio and good mixing in the barrel. With an increasing number of kneading discs, there was an increase in the aspect ratio due to an accumulated level of shear (ID 1 plots of Fig. 7 and 9).

At a low throughput and a high L/S, an increased screw speed assisted early aggregation of the wetted powder, which is reflected by an increase in the fraction of larger granules for all three sample locations (comparing ID 2 plots of Fig. 6 and 8). The addition of more kneading discs further increased the agglomeration level and a successive reduction in the amount of fines. Moreover, at increased screw speed together with an increase in the number of kneading discs, the granules became more spherical (comparing ID 2 plots of Fig. 7 and 9). It can be assumed that increased shear caused a greater consolidation of granules and consequently an increased sphericity, while making squeezed-out liquid available to a further granulate leading to the further shift of the GSD towards larger diameters.

However, when the feed rate was high and the L/S was low, an increase in the screw speed resulted in an early aggregation of the particles with minimal number of kneading discs (comparing ID 3 plots in Fig. 6 and 8). The addition of more kneading discs to the screw caused a reduction in the amount of fines. However, for the configuration with 12 kneading discs there was a reduction in the number density of larger particle sizes at successive sample locations indicating breakage of larger granules induced by the second kneading block (ID 3 plot for 12 kneading discs in Fig. 8). This is likely due to availability of insufficient liquid to make strong bridges between the particles in the granules, which was also reflected in the aspect ratio where no significant change in the shape distribution was observed due to lack of additional particle growth processes (comparing ID 3 plots in Fig. 7 and 9).

The effect of an increase in screw speed at high levels of throughput and L/S was discussed in section 3.2.3. The major contribution of increasing the screw speed at high throughput and L/S was the reduction in granulator torque, without affecting the GSD. This is desirable at manufacturing scale from a productivity point of view where operation at high throughput is a prerequisite.

These comparisons suggest that along with the distributive mixing by the kneading discs, the shear-induced mixing by increasing screw speed is another important factor in mixing. However, increasing the screw speed reduces the mean residence time of the wet powder in the barrel. Hence, a competitive relationship exists between the shear mixing in the barrel and the residence time of the wetted powder, both of which are desired to support granulation rate processes. Except for the granules which are brittle due to lack of sufficient granulation liquid, the shape distribution at high shear remains the same compared to low shear conditions. This suggests that the shape of granules largely depends on the design of the screws and not on the shear level.

4. Conclusions

This study showed that a balanced mixing is important to change the granule characteristics through aggregation and breakage mechanisms along with the consolidation of the particles. The fill ratio in the barrel is an important factor both because it affects the torque required by the granulator drive, and it plays a major role in changing the size and shape of the particles. Increasing throughput is beneficial only when sufficient granulation liquid and shear mixing is present to make strong agglomerates. An increase in throughput causes a higher torque, which can be resolved by increasing the screw speed. The deformation of wet granules is easy and granules with a more uniform shape are produced. A number of competing mechanisms, such as aggregation, consolidation and breakage occur in the process. Although this study provided a detailed insight regarding the process, the experimental data produced only semi-quantitative insight into which of these mechanisms were dominant. Unlike experimental results, where only the collected data are available, mechanistic models are more transparent in the sense that any and all of the intermediate data can be observed after simulation (given a thoroughly validated model is available). Therefore the results obtained from this study will now be used as the basis for the development of a mechanistic model to further improve our understanding of the granulation process in a TSG.

Acknowledgements

Financial support for this research from the BOF (Bijzonder Onderzoeksfonds Universiteit Gent, Research Fund Ghent University) is gratefully acknowledged. The authors would like to offer a note of thanks to Kris Schoeters (GEA Pharma Systems, Collette™, Wommelgem, Belgium) for his support in this endeavour.

References

Dhenge, R. M., Cartwright, J. J., Doughty, D. G., Hounslow, M. J., Salman, A. D., 2011. Twin screw wet granulation: Effect of powder feed rate. Adv. Powder Technol. 22 (2), 162 – 166, special issue of the 6th World Congress on Particle Technology.

Dhenge, R. M., Cartwright, J. J., Hounslow, M. J., Salman, A. D., 2012. Twin screw granulation: Steps in granule growth. Int. J. Pharm. 438 (1-2), 20–32.

Djuric, D., Van Melkebeke, B., Kleinebudde, P., Remon, J. P., Vervaet, C., 2009. Comparison of two twin-screw extruders for continuous granulation. Eur. J. Pharm. Biopharm. 71 (1), 155–160.

El Hagrasy, A. S., Litster, J. D., 2013. Granulation rate processes in the kneading elements of a twin screw granulator. AIChE J. 59 (11), 4100–4115.

Ennis, B. J., 2010. Theory of Granulation: An Engineering Perspective. In: Handbook of Pharmaceutical Granulation Technology. pp. 6–58.

Fonteyne, M., Soares, S., Vercruysse, J., Peeters, E., Burggraeve, A., Vervaet, C., Remon, J. P., Sandler, N., De Beer, T., 2012. Prediction of quality attributes of continuously produced granules using complementary pat tools. Eur. J. Pharm. Biopharm. 82 (2), 429–436.

Kumar, A., Gernaey, K. V., De Beer, T., Nopens, I., 2013. Model-based analysis of high shear wet granulation from batch to continuous processes in pharmaceutical production – a critical review. Eur. J. Pharm. Biopharm. 85 (3, Part B), 814 – 832.

Kumar, A., Vercruysse, J., Toiviainen, M., Panouillot, P.-E., Juuti, M., Vanhoorne, V., Vervaet, C., Remon, J. P., Gernaey, K. V., Beer, T. D., et al., 2014. Mixing and transport during pharmaceutical twin-screw wet granulation: experimental analysis via chemical imaging. Eur. J. Pharm. Biopharm.

Lee, K. T., Ingram, A., Rowson, N. A., Aug. 2012. Twin screw wet granulation: the study of a continuous twin screw granulator using Positron Emission Particle Tracking (PEPT) technique. Eur. J. Pharm. Biopharm. 81 (3), 666–73.

Lee, K. T., Ingram, A., Rowson, N. A., 2013. Comparison of granule properties produced using Twin Screw Extruder and High Shear Mixer: A step towards understanding the mechanism of twin screw wet granulation. Powder Technol. 238, 91–98.

Litster, J., Ennis, B., 2004. The science and engineering of granulation processes. Vol. 15. Springer.

Van Melkebeke, B., Vervaet, C., Remon, J. P., 2008. Validation of a continuous granulation process using a twin-screw extruder. Int. J. Pharm. 356 (1-2), 224–230.

Vercruysse, J., Córdoba Díaz, D., Peeters, E., Fonteyne, M., Delaet, U., Van Assche, I., De Beer, T., Remon, J. P., Vervaet, C., 2012. Continuous twin screw granulation: Influence of process variables on granule and tablet quality. Eur. J. Pharm. Biopharm. 82 (1), 205–211.

Vercruysse, J., Toiviainen, M., Fonteyne, M., Helkimo, N., Ketolainen, J., Juuti, M., Delaet, U., Assche, I. V., Remon, J. P., Vervaet, C., De Beer, T., 2013. Visualization and understanding of the granulation liquid mixing and distribution during continuous twin screw granulation using NIR chemical imaging. Eur. J. Pharm. Biopharm. 86 (3), 383–392.

Vervaet, C., Remon, J. P., 2005. Continuous granulation in the pharmaceutical industry. Chem. Eng. Sci. 60 (14), 3949–3957.

List of Figures

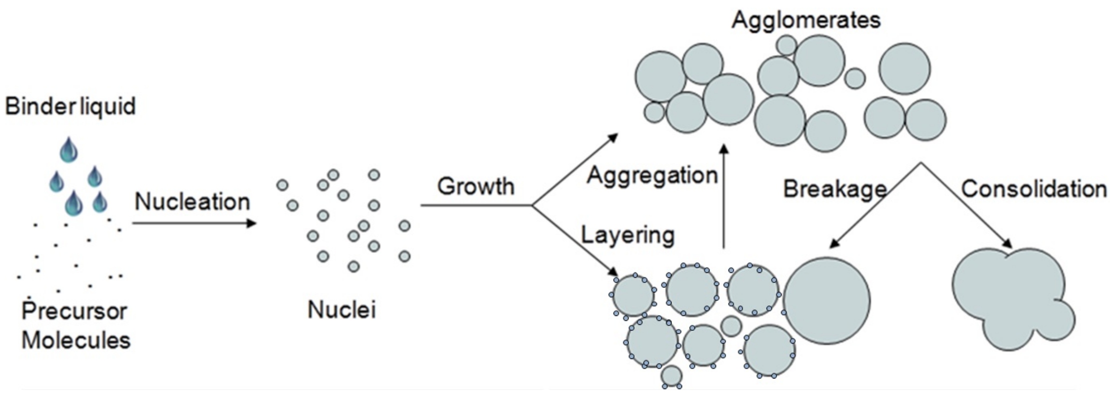

Figure 1: Schematic presentation of the wet granulation process.

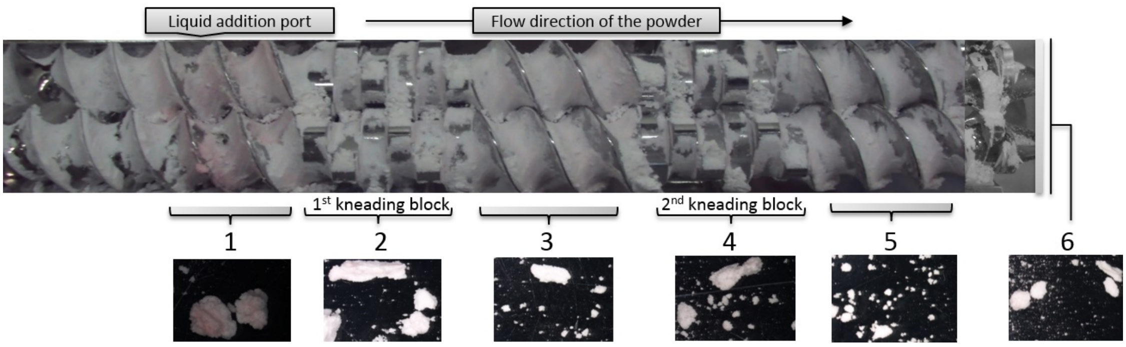

Figure 2: Screw configuration with 12 kneading discs (2 blocks) used in the twin screw granulator during the study. Sampling locations along the screw length: [1] before first kneading block, [2] on the first kneading block [3] between first and second kneading block, [4] on the second kneading block [5] after second kneading block, [6] outlet of the granulator.

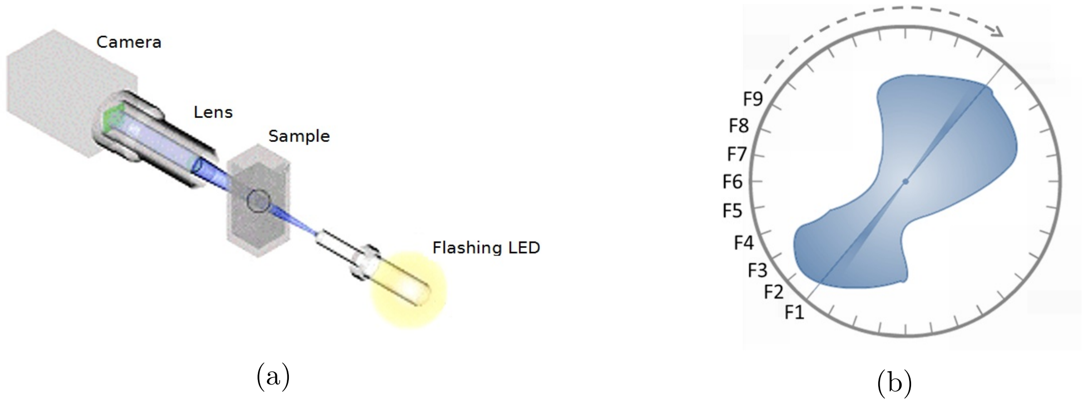

Figure 3: (a) Principle of the dynamic image analysis technique. The shape and size of the granule are determined based on the imaged formed by the LED flashing light passing directly through the sample and captured by the camera. (b) The Ferret diameters provide information on the size (average Ferret diameter), give deep insight into the granules morphology (minimum Ferret and maximum Ferret) and serve as a basis for the calculation of the aspect ratio.

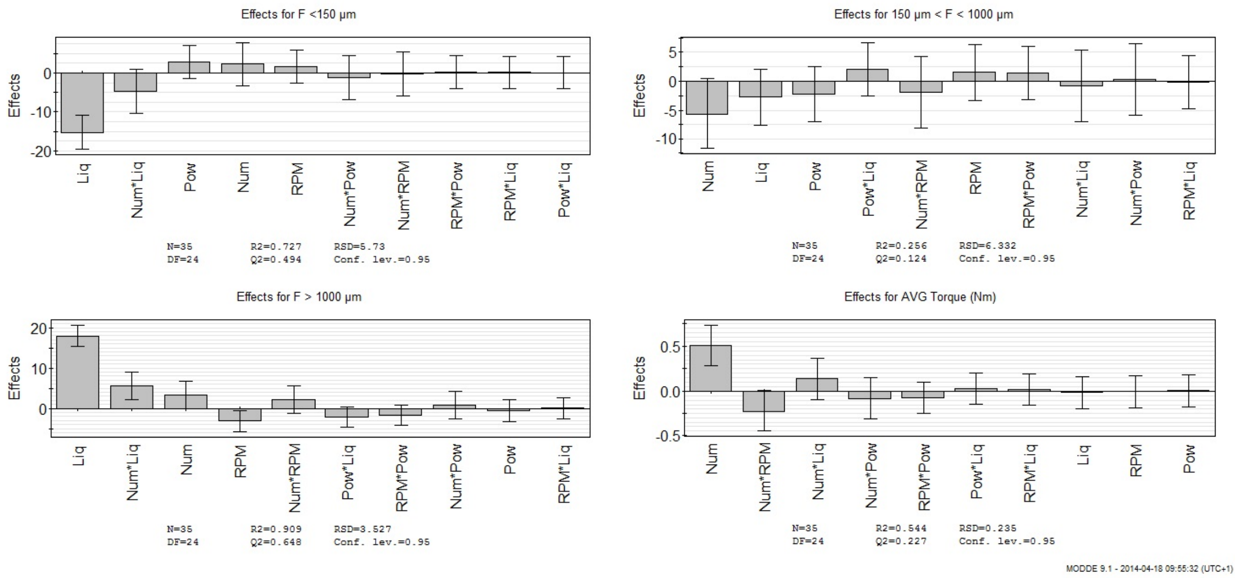

Figure 4: Effect plots of the partial least squares (PLS) models showing the mean responses of number of kneading discs (Num), screw speed (Scr) [500-900 rpm], throughput (Pow) [10-25 kg/h] and liquid-solid ratio (Liq) [4.58-6.72%] on the size fractions (F) defined as fines (F < 150 µm), fraction of interest for tableting (150 µm< F< 1000 µm) and oversized granules (F>1000 µm) and the measured torque.

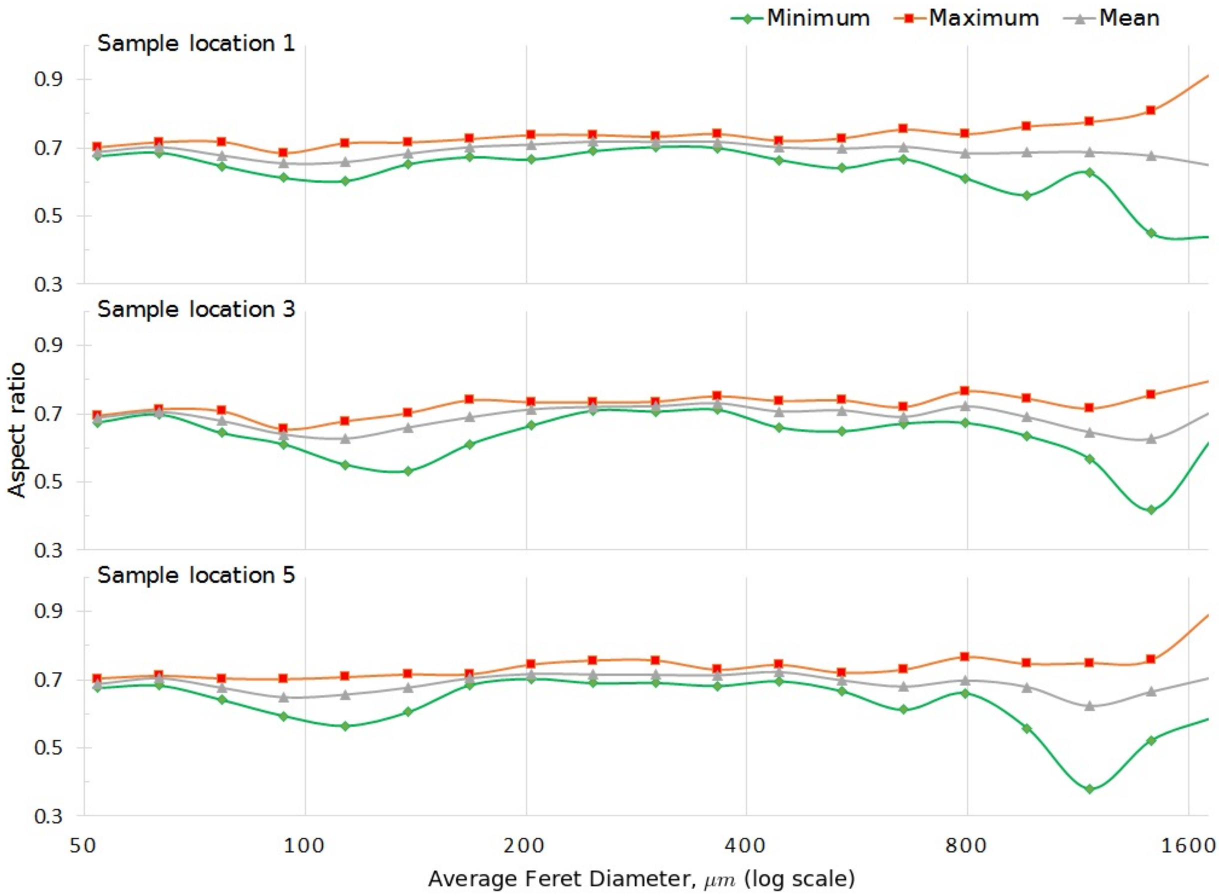

Figure 5: Mean, maximum and minimum aspect ratios vs. mean Feret diameter of the granules in the range of 50 to 1600 µm (log scale, x-axis) at location 1 (top subplot), location 3 (middle subplot) and location 5 (bottom subplot) in barrel for the runs performed at different throughputs (10, 25 kg/h), liquid-to-solid ratio (4.58, 6.72% (w/w)), screw speed (500, 900 rpm) and number of kneading discs (4, 12).

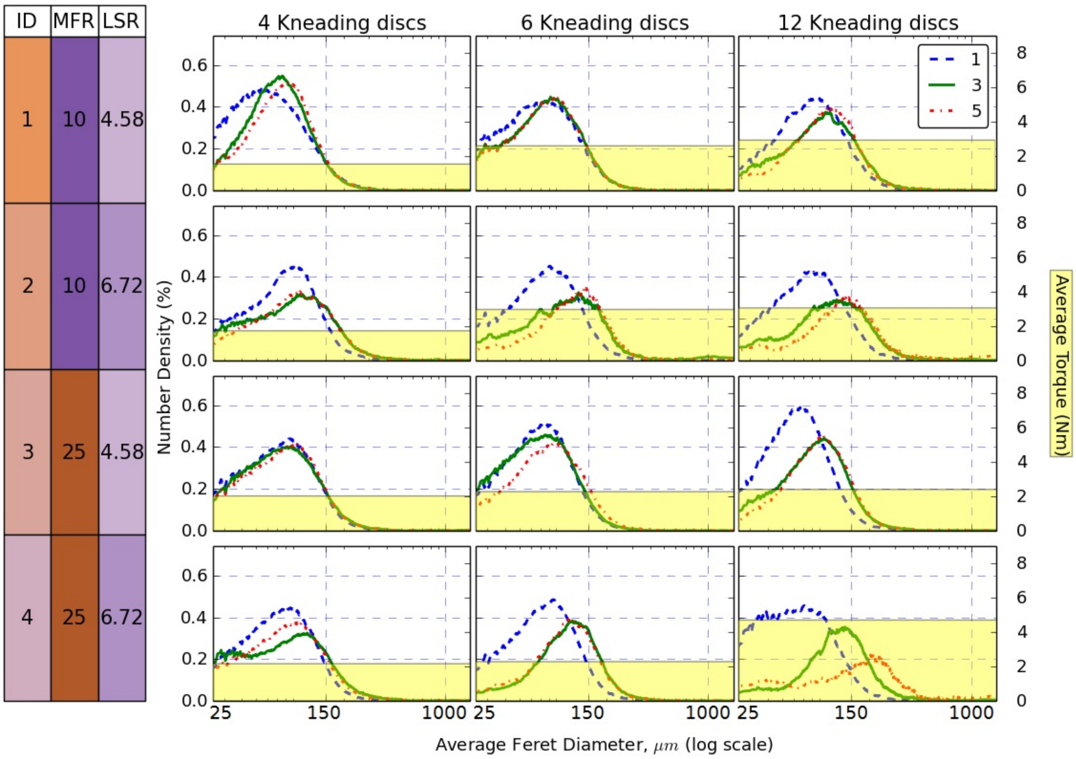

Figure 6: Number density of the granules (primary y-axis) having an average Feret diameter in the range of 50 to 1500 µm (log scale, shared x-axis) and torque level (secondary y-axis) at different throughputs (10-25 kg/h), liquid-to-solid ratio (4.58-6.72% (w/w)) at low screw speed (500 rpm) [ID: experiment ID, MFR: throughput (kg/h), LSR: liquid-solid ratio (%)].

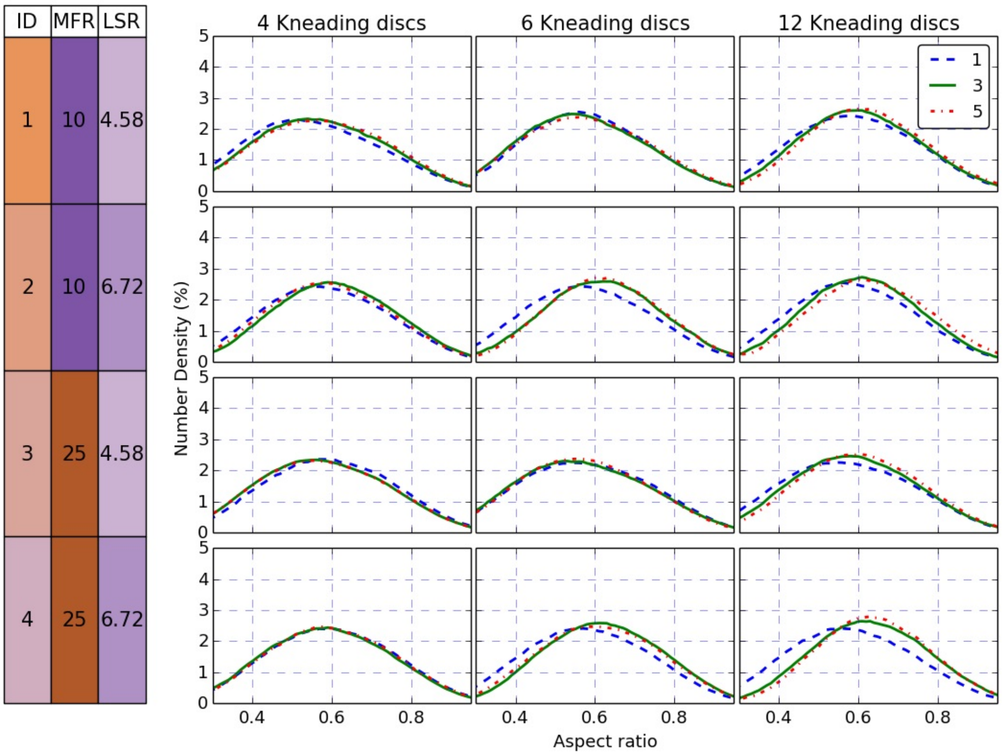

Figure 7: Number density of the granules (primary y-axis) having an aspect ratio in the range of 0.3 to 1 (shared x-axis) at a different throughput (10-25 kg/h), liquid-to-solid ratio (4.58-6.72% (w/w)) at low screw speed (500 rpm) [ID: experiment ID, MFR: throughput (kg/h), LSR: liquid-solid ratio (%)].

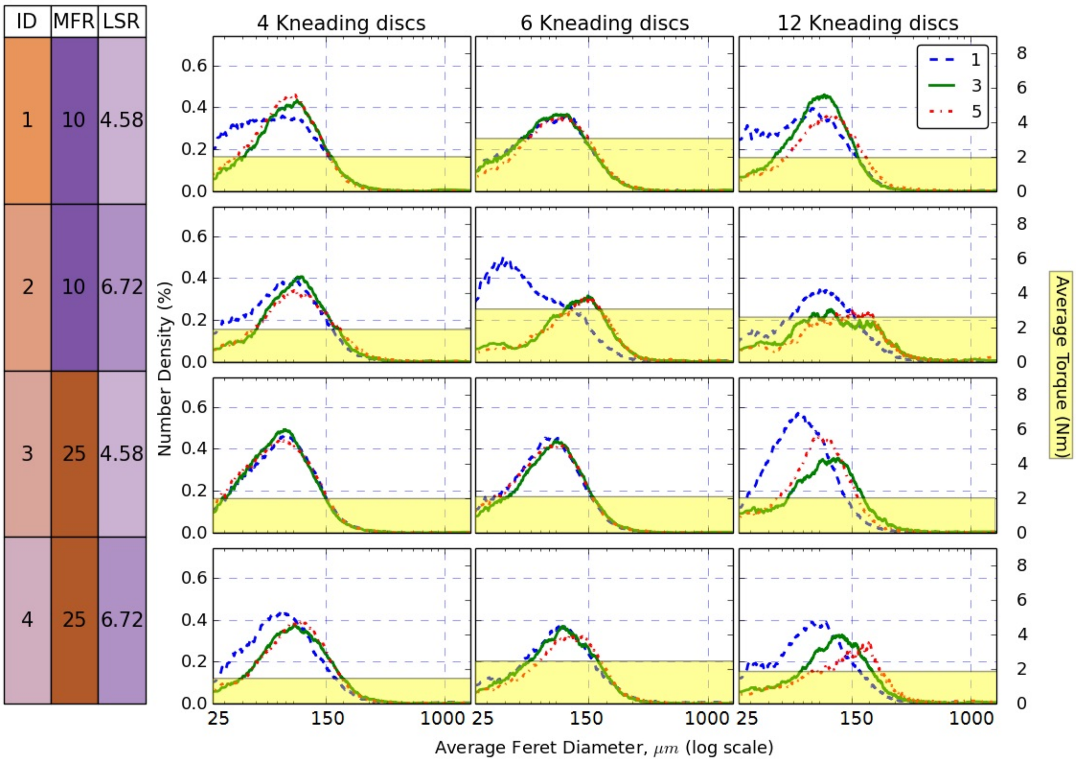

Figure 8: Number density of the granules (primary y-axis) having an average Feret diameter in the range of 50 to 1500 µm (log scale, shared x-axis) and torque level (secondary y-axis) at different throughputs (10-25 kg/h), liquid-to-solid ratio (4.58-6.72% (w/w)) at high screw speed (900 rpm) [ID: experiment ID, MFR: throughput (kg/h), LSR: liquid-solid ratio (%)].

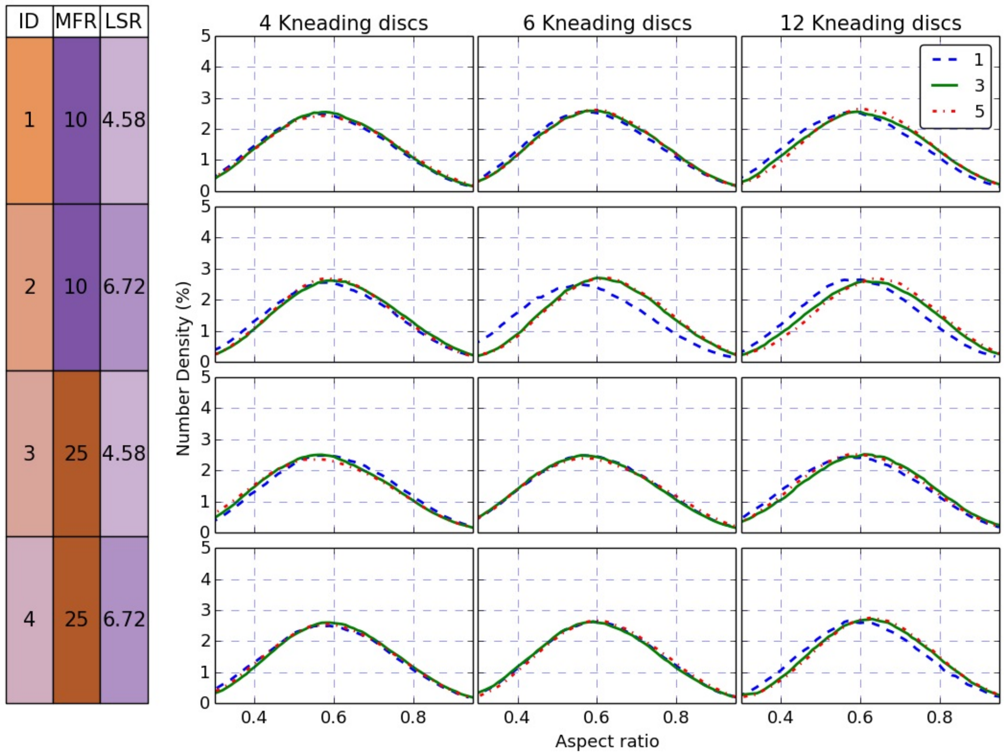

Figure 9: Number density of the granules (primary y-axis) having an aspect ratio in the range of 0.3 to 1 (shared x-axis) at different throughputs (10-25 kg/h), liquid-to-solid ratio (4.58-6.72% (w/w)) at low screw speed (900 rpm) [ID: experiment ID, MFR: throughput (kg/h), LSR: liquid-solid ratio (%)].

List of Tables

Table 1: Overview of experimental design runs: factor variables (number of kneading discs, screw speed, throughput and liquid-solid ratio) and responses (Torque, F < 150 µm (defined as fines), 150 µm<F<1000 µm (fraction of interest for tabletting) and F>1000 µm (defined as oversized) granules).

Run Order	**Number of kneading discs (-)**	**Screw speed (RPM)**	**Throughput (Kg/h)**	**L/S ratio (%)**	**Torque (N-m)**	**F<150 µm (%)**	**150-1000 µm (%)**	**F>1000 µm (%)**
1	2	500	10	4.58	34.95	42.19	22.86	1.38
2	4	500	10	4.58	40.66	37.95	21.39	1.84
3	6	500	10	4.58	38.28	43.77	17.95	2.59
4	12	500	10	4.58	43.2	37.87	18.93	2.92
5	2	900	10	4.58	37.86	46.02	16.11	1.25
6	4	900	10	4.58	43.12	39.53	17.34	2.00
7	6	900	10	4.58	42.78	39.25	17.96	3.06
8	12	900	10	4.58	40.68	37.62	21.7	1.95
9	2	500	25	4.58	36.25	35.66	28.09	1.30
10	4	500	25	4.58	45.79	31.01	23.19	2.02
11	6	500	25	4.58	42.52	37.54	19.93	2.27
12	12	500	25	4.58	45.41	34.69	19.91	2.4
13	2	900	25	4.58	39.87	38.88	21.25	1.55
14	4	900	25	4.58	45.87	36.15	17.98	1.98
15	6	900	25	4.58	43.9	40.89	15.21	2.09
16	12	900	25	4.58	45.07	35.89	19.04	2.02
17	2	500	10	6.72	22.29	39.62	38.10	0.92
18	4	500	10	6.72	22.55	35.65	41.80	1.73
19	6	500	10	6.72	28.49	32.80	38.71	2.97
20	12	500	10	6.72	23.80	34.84	41.36	3.06
21	2	900	10	6.72	23.56	39.75	36.7	1.44
22	4	900	10	6.72	25.70	33.27	41.04	1.89
23	6	900	10	6.72	29.04	34.82	36.15	3.07
24	12	900	10	6.72	22.19	35.15	42.66	2.6
25	2	500	25	6.72	26.14	36.3	37.56	1.24
26	4	500	25	6.72	29.37	32.43	38.21	2.16
27	6	500	25	6.72	33.58	33.71	32.71	2.28
28	12	500	25	6.72	16.10	34.46	49.43	4.7
29	2	900	25	6.72	26.01	44.26	29.73	1.54
30	4	900	25	6.72	30.72	34.44	34.84	1.46
31	6	900	25	6.72	32.58	37.62	29.79	2.46
32	12	900	25	6.72	26.25	31.31	42.44	1.86
33	4	700	17.5	6	22.58	55.90	21.52	1.33
34	4	700	17.5	6	18.52	53.03	28.45	1.32
35	4	700	17.5	6	20.59	55.50	23.92	1.24